SOME IMPROVEMENTS OF THE LSD OPTICAL SYSTEM

CERN-LSD Group (presented by K.K. Geissler)

SUMMARY

The overall efficiency of the optical system of the LSD has been reviewed with reference to its influence on the signal-to-noise ratio of the track detector output signal and found to be not optimal. The improvements undertaken are aimed at raising the quality of the output signal of the photomultipliers by supplying them with the maximum possible light intensity, thus reducing the influence of the Schottky shot noise on the signal quality to a tolerable level. This was done using two types of mirror coatings which are radically different from the existing ones. Further measures consisted of changing the type of cone/periscope PM, raising the Xenon lamp current to its rated value and using specially selected filters.

The definition of the spectral transmittance curves of the coatings was based on information given by the lens manufacturer SCHNEIDER & Co. about the chromatic aberrations of the projection lens, as they occur in the LSD machine.

The theoretical forecast for the result of this improvement study is a factor of 2,5 for the S/N ratio of the track signal and a factor of about 3 for the S/N ratio of the fiducial signal.

INTRODUCTION

In the course of a program to convert the "Test CP" into LSD2-Pollux, the somewhat noisy output signal from the cone/periscope assembly photomultiplier ("track PM") was found to be partly due to the track detector PM XP 1110 in use at that time. It was decided to replace it by the type XP 1002 which has a S-20 trialkali photocathode.

The study about optimisation revealed furthermore that the existing arrangement favoured the fiducial detector PM to an unduly high extent at the cost of the track detector PM. Some details show this:

1. Slit surfaces
   - dimensions of track slit: 1000µ × 50µ;
   - dimensions of fiducial slit: 3000µ × 100µ;

   i.e. a ratio of 1:6

2. Light guides
   - 300 + 900mm for tracks; transmission 30%;
   - 500mm for fiducials; transmission 55%;

   i.e. a ratio of 1:1,8

3. Splitting ratio of large mirror
   - reflectance at 480nm (for track detector)= 40%
   - transmittance at 480nm (for fiducial detector)= 60%

   i.e. a ratio of 1:1,5

This results in a total "favouring" factor of

$$1: (6 \times 1{,}8 \times 1{,}5) = 1:16$$

as far as the luminous flux upon the two PMs is concerned.

A direct consequence of this large factor was the following. The 8 fiducial PMs and the single track PM were supplied by a common high voltage source. When the Xenon lamp current was raised in order to improve the track signal quality, the fiducial PMs very soon were overcharged. Consequently, the lamp current was set at 19A, far below the rated value of 25A.

The main task yet was the determination of the coatings for the two splitter mirrors. These are:

1. The "small splitter", which is 150mm in diameter, 15 mm thick and splits away the light for the operator's table;

2. The "large splitter", which is 400mm in diameter, 30mm thick and splits the light between cone/periscope image plane and fiducials/TV image plane.

TRANSMISSION CHARACTERISTICS OF THE OPTICS AND PM RESPONSE

From the point of view of PM sensitivity the different optical devices used in the LSD are "hostile". This is not bad engineering but a natural fact and shall be outlined in some detail.

The spectral response curves of the S-11 and S-20 photocathodes (shown in **fig.** 1) peak at wavelengths ranging from 380nm to 420nm. The standard Cs_3 Sb-O composition of the S-11 shows a steep descent towards longer wavelengths, while the trialkali composition Na_2 KSb-Cs of the S-20 has lower values of the photoelectric work function than the S-11 and thus shows an appreciable sensitivity in the red spectral region (50% at 600nm compared to 12% of the S-11; see fig. 1). It is logical to concentrate on the blue and violet spectral region when designing an optical device for use with a photomultiplier. The relative spectral transmission curves of the optical components in the LSD (fig. 2) show increasing absorption towards shorter wavelengths. Fig. 3 shows the overall spectral transmission curve of all optical components which are common to both image planes on either side of the large splitter. The light guides are taken with their respective PMs to form the "detector units".

In order to obtain information upon which to base a decision about the splitting ratio, the relative spectral distribution of the radiant output of the Xenon lamp has been evaluated from OSRAM calibration curves and is plotted in fig. 4. The total product of

Xenon lamp	(fig. 4)
times light guide transmission	(fig. 2)

times PM spectral sensitivity (fig. 1)

times overall transmission (fig. 3)

yields the two curves in fig. 5, which show the relative spectral response of the two PMs involved. These curves are "maximum curves" in the sense that they are obtained

- for the fiducial PM with small splitter R = 100%
  and large splitter R = 0%
- for the track PM with small splitter R = 100%
  and large splitter R = 100%

Both PMs show peak response at 470nm. The peaks are due to the 470nm peak in the output power curve of the Xenon lamp. The absorption and reflection losses encountered in the combination of a 300mm and a 900mm light guide in front of the track PM are obviously responsible for the remarkably inferior response of the track PM, at least in the region of peak response.

There is still one peculiarity to be explained that would help in the understanding of the characteristic behaviour of a PM which is illuminated with light of a certain wavelength.

The radiant cathode sensitivity $E(\lambda)$ in mA/watt is defined as

$$E(\lambda) = \frac{I_k}{P} \approx \lambda . Q(\lambda)$$

that is, photocurrent per radiant power P having a wavelength λ. Thus $E(\lambda)$ is valid information only for particular wavelengths, since the radiant power P as well as the quantum efficiency $Q(\lambda)$ have to be specified for these wavelengths.

It is customary for photocathode sensitivities to be quoted as luminous sensitivity in units of µA/lumen, since the lumen is related to the human eye and covers a wide spectral range.

A source with an emission spectrum $W(\lambda)$ gives rise to a luminous flux of dF lumens in the wavelength region λ to $\lambda+d\lambda$:

$$dF \sim V(\lambda)\ W(\lambda)\ d\lambda$$

$V(\lambda)$ is the relative response of the standard eye and provides the reference to the human eye.

When a light source with the emission spectrum $W(\lambda)$ cited above irradiates a photosensitive surface with a flux in the wavelength region λ to $\lambda+d\lambda$, the current di_k would be:

$$di_k \sim E(\lambda)W(\lambda)d\lambda$$

or

$$di_k \sim \lambda.Q(\lambda).W(\lambda)d\lambda$$

In our case the value $W(\lambda)$ is obviously given by the spectral distribution curve of the Xenon lamp (figure 4) whereas the term $\lambda.Q(\lambda)$ is given by the relative spectral response curves in fig. 1. It is thus clear that the PM output current is proportional to the area under the spectral sensitivity curve in the S versus λ plot shown in fig. 5.

Finally, the actual values of cathode sensitivities as given in the data sheets were obtained using a tungsten ribbon lamp at 2857°K, which resembles very closely a black-body radiator, whose emission data $W(\lambda)$ are tabulated.

The expression for the cathode sensitivity S in μA/lumen

$$S = \frac{C_1 \int E(\lambda)\ W(\lambda)\ d\lambda}{C_2 \int V(\lambda)\ W(\lambda)\ d\lambda}$$

may be evaluated by numerical integration using calibrated values of $E(\lambda)$ for a particular tube and tabulated data for $V(\lambda)$.

The statement of cathode sensitivity in μA/lumen makes it difficult to compare two cathodes having appreciably different spectral

responses. In particular, the fact that the emission spectrum for a 2857°K black body peaks at a wavelength of 1000nm (1 micron) may result in a disproportionate increase in photosensitivity for a small extension of the long wavenlength tail of the quantum efficiency curve. The two types of PM used in the LSD are a good illustration of this fact:

	XP 1110	XP 1002	
radiant sensitivity at 420nm,	60	70	mA/watt
luminous sensitivity	60	150	µA/lumen

PERFORMANCE OF THE SCHNEIDER REPRO-CLARON

A particular study of the degradation of image quality due to geometrical and chromatic aberrations introduced by the 4,5mm thick glass plate in the film gate seemed appropriate as well. These aberrations are likely to occur since the spherical abberations are a function of the index of refraction which in turn varies with the wavelength of the light used for projection.

The manufacturer of the lens, J. SCHNEIDER, Bad Kreuznach, helped by running a special computer program and supplied all relevant data in the form of a computer print-out from which the following comments are extracted (examples are shown in figs 6 and 7).

For a 0% - 100% step function in the object plane the program computed the energy distribution in the image plane for a magnification of 2.8. This was given for both sagittal and meridional (tangential) orientation of the step function with respect to the optical axis and for varying

- image plane positions ($\Delta s'$ = 0, -2,5 and -5mm)
- colours (blue, 480nm; green, 546nm; red, 644nm)
- off-axis distances in the image plane (0,40, 80, 120, 160mm).

The sketch shall illustrate this:

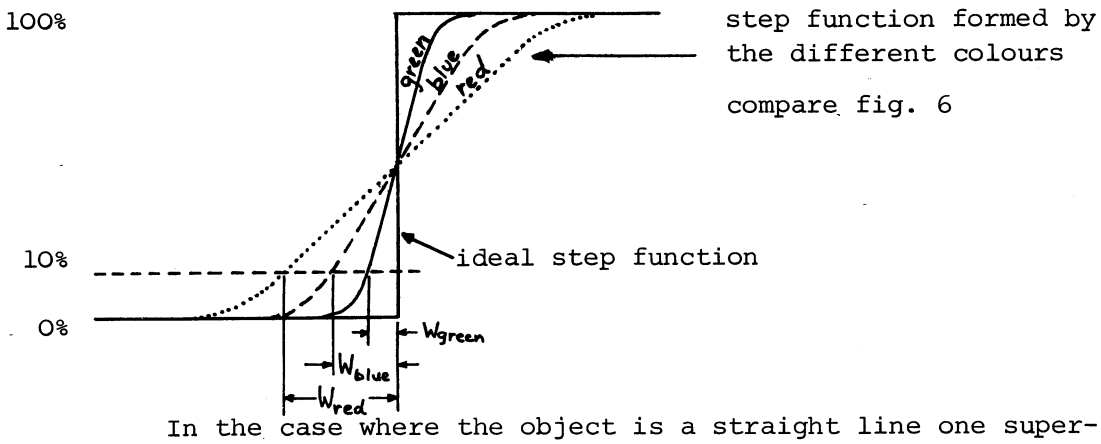

In the case where the object is a straight line one superposes this step function with its inverse function, as shown by the solid and dashed lines in fig. 8a. When overlapped properly so that the ideal width W_i in the image plane is equal to object width times magnification, one can obtain the real image by multiplying the appropriate distribution curves (as shown in fig. 8a by the dotted curve).

A certain "smear-out" or broadening of the line image can be seen. To extract useful information about this "smear-out", the distribution curves have been cut at 10% height and thus the value W was found, which is proportional to the total width (at 10% height) since the ideal width W_i is constant, see fig. 8a. This value W is evidently a representative measure of the quality and sharpness of the projected image under the various conditions involved.

It should be mentioned that the data in the computer output is derived by purely geometrical ray computing and thus is of only limited significance, although adequate for our purposes. The interpretation of the results is restricted to blue and green light, where the PMs are most sensitive. Furthermore, only sagittal lines are studied since these are equivalent to radially oriented tracks from a vertex. In the particular case of the fiducial arms, some reference to the related case of meridional oriented lines will be made.

There are two regions of chief interest:

(i) vertex region, i.e. optical axis

(ii) fiducial region, i.e. 160mm off-axis

(i) The interest stems from the fact that in this region the measurements of track ionisation are made and therefore highest image quality is needed.

(ii) The fiducial region is a very critical one:

- it is far away from the optical axis;
- the fiducial arms are not radially oriented, but under angles from 35° to 65° referred to a radial line. This introduces an appreciable amount of aberration coming from the "meridional case". Figs 6 and 7 will illustrate this. The right hand side diagram in fig. 7 shows the original information which indicates a 40μ displacement at 50% step height for the tangentially oriented edge image, while the dotted curve in fig. 8b shows the energy distribution for a 60μ thick line image (tangentially oriented) composed in the manner described above.
- The large 45° splitter mirror of 30mm thickness created additional coma and chromatic aberrations. These particular non-symmetrical conditions are currently under study at SCHNEIDER. Definite results are not yet available, but preliminary information indicates that the coma effect is larger than the chromatic aberrations.

The information about the performance of the Repro-Claron supplied by SCHNEIDER & Co is plotted in fig. 9a. For the two wavelengths blue (480nm, dashed lines) and green (546nm, solid lines) the "pulse width W" is plotted versus different focal plane positions $\Delta s'$. The different off-axis distances (in the image plane) are inserted in the curves as a parameter. The pulse width W is to be taken in a relative sense and serves only for the purpose of comparison.

W is taken arbitrarily at 10% step height and does not relate to any absolute value. For instance, if it were taken at 50% step height, W would be equal to zero.

Evidently the highest line image quality is obtained with green light. Three cases may be distinguished:

(1) At $\Delta s' = -2{,}5$mm the smallest line image is given on the optical axis (0mm) but the width increases with increasing radius of the spiral, up to 40µ for 160mm off-axis distance.

(2) At $\Delta s' = -4$mm the initial width is larger but there is no variation of width for green light from 0 to 80mm and for blue light only modest variation occurs. For greater radii the width increases but in a less pronounced fashion.

(3) At $\Delta s' = -5$mm the variation of width over the entire range of off-axis distances is smallest, but the initial width is double that of case 1.

The general requirements to be fulfilled for track images are:

(1) Sharpness;
(2) High signal-to-noise ratio, i.e. high light level.

Comments on these two points are:

(1a) Sharpest images (for ionisation measurements) are needed only for image plane off-axis distances 0 to 40mm, for larger distances the requirements are less stringent.

(2a) More light for the track PM means less relative noise and thus clearer, more reliable pulses, even when track images are slightly broader than in the optimal case.

A compromise has been found with light of 500nm wavelength (blue-green) that yields for the track image a reasonably small width around the optical axis (0 to 40mm) as well as modest increase for larger distances (compare fig. 9b and the two vertical arrows there).

Logically the wavelength region around 470nm will now be used to illuminate the fiducial detectors. The V-slits of the pick-up system are at fixed positions so that no pulse width variations will occur. The best image plane will be set for each V-slit independently. The dashed line in fig. 9b indicates that at $\Delta s' = -6,5$mm the pulse width W for the fiducial marks may be the same as for the tracks. Of course, the influence of the large 45^{o} splitter mirror (coma, chromatic aberration) was not taken into account, this will change the entire situation as may be deduced from fig. 8b.

THE MIRROR COATINGS

When it comes to specifying the spectral characteristic of the mirror coatings one should remember that it is the area under the spectral sensitivity curve of the track detector unit that counts, since it is directly related to PM output current.

Now we are obliged to operate the track detector unit within a narrow spectral region. It is therefore logical to split the available light spectrally and not (as is normal) to split the intensity. In other words: The mirror coating must have the characteristics of a bandpass frequency filter, whose reflectance is ideally 100% for the specified spectral region and whose transmittance is ideally 100% for the rest of the spectrum.

For obvious reasons of human engineering this cannot be applied to the small splitter which transmits the light to the operator's table. In this case a more or less neutral splitter has to be specified.

In close cooperation with BALZERS, Liechtenstein the two types of coatings were specified and manufactured by them. The small splitter is treated on the first surface with a standard TRANSFLEX TF-TS2T-65 coating and with a "short IRALIN" as antireflection coating on the second surface. "Short" in this context means that the standard IRALIN spectral curve has been shifted by 30 to 40nm towards shorter wavelengths.

The large splitter was coated with a specially developed type of many-layer dielectric coating which is based on the standard type "DC GRÜN", but differs in that it is centered at 505nm and reflects as much as 98% of the light at this wavelength. The "full-width-half-magnitude" value is about 60nm. For the other spectral region of interest, 400 to 470nm (fiducials), the transmittance is 80% on average with a peak transmittance of 91% for 430 to 455nm. From 560nm to the red end of the spectrum the transmittance is about 90% (TV camera). These curves are shown in fig. 10, together with the curves for the hitherto applied oxide coated neutral splitters. The second surface of the large splitter is coated with a "short" GEDO type double-layer antireflection coating, since the multi-layer type IRALIN would have been extremely difficult to apply homogenously on such a large substrate.

Finally, the mirror strip inside the cone has been given another coating. Instead of ALFLEX A (R = 88% at 500nm) a SILFLEX coating with protective SIO coating (R = 98% at 500nm) was applied.

RESULTS

The final results obtained by taking into account the reflectances and transmittances of the two new splitter mirrors are given in the following figures.

The solid curve in fig. 11 gives the relative spectral sensitivity of the track PM (XP 1002, S-20), while the dashed curve indicates the actual spectral response of the track PM (XP 1110, S-11) in LSD1. The dashed curve was calculated in the same way as the solid curve, using the R/T ratio of the old mirror set and the lower relative radiant output of the Xenon lamp. The dotted curve will be mentioned in the section Outlook. There is no need to use a colour filter - the coating of the large splitter behaves already as expected as a very efficient broadband interference filter.

It is evident that the new PM response will result in a remarkable increase in output current and thus in a much less noisy output signal than that given by the area under the dashed curve. The signal-to-noise ratio will improve by a factor of 2 or more.

The solid curve in fig. 12 shows the relative spectral sensitivity of the fiducial PM (XP 1110, S-11) and again the actual operating conditions are given by the dashed curve. Here as well a striking increase in PM output current is to be seen. Hitherto a SPECIVEX 540 B filter was used. At the wavelength of its peak transmission (540nm) the relative sensitivity of the XP 1110 is already as low as 45%. Due to the favouring of the fiducial/TV image plane it was not obvious that the subsequent attenuation of the surplus light by the filter was at the cost of the cone/periscope image plane which thus responded with a poor signal-to-noise ratio.

The dotted continuation of the solid curve is that portion which will be cut away by the filter FITC-3 special, developed by BALZERS and shown in fig. 15. Since the aberrations introduced by the large splitter are not yet known, it will be decided by direct experiment on the machine whether this filter is to be applied or not.

Two curves for the final relative spectral sensitivity of the vidicon are shown in fig. 13. The reasoning is the same as for

the fiducial filter. So once more, the unknown chromatic aberrations introduced by the large splitter leave the decision to a direct experiment on the LSD, as to whether a sharper image on the TV is produced by green light of 550nm (using the BALZERS filter FILTRAFLEX DT GRÜN, see fig. 15) or by blue light of 470nm (using the fiducial filter FITC-3 special see fig. 15). Both methods are acceptable, the relative spectral sensitivity of the vidicon being 70% for blue and 100% for green light.

The two circles in fig. 9a marked "TV" indicate for the pulse width W a best value of 10µ for the green light (540nm) and 20µ for the blue light (480nm).

The relative spectral distribution of the light falling through the small splitter upon the operator's table is shown in fig. 14. A first test with a small glass plate sample of TRANSFLEX-65 showed better results than would have been expected from fig. 14. The reason is perhaps that compared with the relative spectral sensitivity of the human eye the two peaks at 470nm and 620nm are sensed with 10% and 40% only of the relative response of the eye. The light on the projection table appears slightly reddish instead of snow white and that is all. This appears to be acceptable since the operator did not complain about eye strain.

OUTLOOK

In the course of this study it became apparent that further improvements are possible, which would not necessitate any change in the design or construction of the machine.

The first case where an appreciable improvement in performance could still be gained concerns again the large splitter mirror. Some brief details shall explain this.

A dielectric mirror is produced by stacking optical interference films in such a way that alternate layers of dielectric materials with low refractive index and high refractive index are deposited. This particular coating is called a quarter-wave stack because the films all have the same optical thickness of a quarter of a wavelength at the "tuned" wavelength. The spectral region of high reflectance of the coating is called a "stopband".

There are three characteristic points of some importance with such a stopband:

(1) The centre wavelength can be chosen at will, since the optical thickness is controlled accordingly during the evaporation process.

(2) Adding extra pairs of layers of the two dielectric materials increases the maximum reflectance, but the spectral width of the stopband is unchanged.

(3) The spectral width of the stopband depends only on the refractive index of the two films that are used in the stack and is independent of the number of layers.

After discussion with BALZERS it became clear that by applying a material with a different high refractive index the spectral width of the stopband on the large splitter could be increased from 60nm to 90nm. This leads to the first proposal for eventual further improvements of the track PM output signal:

- A stopband from 480nm to 570nm. This spectral width would include the green portion of the spectrum which is found to be best suited from the point of view of image quality.

The second proposal concerns an optical element which did not seem to promise much improvement: the light guides. Replacing the ordinary light guides currently used in the cone/periscope system by SCHOTT ZM2 4x4mm image guides for instance would result in an appreciably

higher luminous flux. An ordinary short fiber light guide has a transmittance not higher than 60%, mainly due to reflection losses at the entrance and exit surface and the "filling factor" encountered when putting loose fibers together into a bundle. The greater packing density of the regularly structured image guide results in a higher filling factor. Instead of the existing transmittance of the 300mm + 900mm combination

$$60\% \times 50\% = 30\%$$

one would find

$$75\% \times 60\% = 45\%.$$

This is equivalent to 50% more light for the track PM.

By combining these two effects the dotted response curve in fig. 11 was obtained.

THE IMPORTANCE OF ANTIREFLECTION COATINGS

On the second surface of both the small and the large splitter mirror an antireflection coating has been deposited. Why do these coatings have to be "short" coatings ? Alternatively, why are their spectral reflectance curves shifted towards the blue end of the spectrum ?

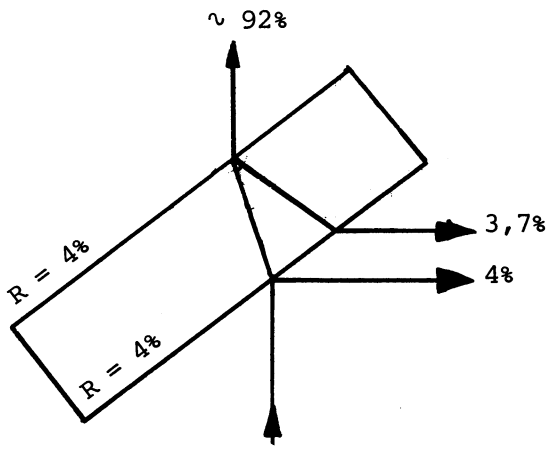

This simple sketch demonstrates for an uncoated glass plate that reflection from first and second surface is of almost equal intensity.

The principal point with antireflection coatings is therefore: They must be of highest efficiency, i.e. minimum reflectance in that particular spectral region, where the first surface coating is of low reflectance. In other words: The parasitic light of the second surface ghost image cannot penetrate the first surface coating when its reflectance is high.

These are exactly the conditions we meet with the large splitter. The following table shows values extracted from figs 10 and 16.

TABLE 1

wavelength	450	470	500	620	nm
small splitter, R_S	50	60	65	50	%
large splitter, R_L	10	20	98	10	%
IRALIN, r_s	0.1	0.12	0.16	0.14	%
GEDO, r_L	0.6	0.6	0.65	1.2	%

Fig. 17 sketches the situation in the LSD machines and shows the fractions of the normalised incident light intensity appearing at the various places.

For the case of the track PM the attenuation of the ghost images by the AR coatings is shown in table 2. Of real importance for the cone/periscope system are the "blue and red ghosts" from the large splitter (1.72% and 1.72%), where R_L is only 10% !

The results are weighted with appropriate S values from fig. 5 and are thus directly related to the final spectral sensitivity curve of the track PM in fig. 11.

TABLE 2

wavelength	450	470	500	620	nm
no AR coatings	1.72	1.67	0.5	1.72	%
with AR coatings	0.27	0.25	0.05	0.5	%
weight S	9	15	10	6	%
final "ghost intensity"	0.02	0.04	0.004	0.03	%

Referred to a 100% spectral response of the track PM due to the primary image the response due to the parasitic light from the ghost image could be reduced by the AR coatings to 0.8%.

FIGURE CAPTIONS

Fig. 1 Relative spectral response curves for the S-11 and S-20 PM photocathode and the vidicon.

Fig. 2 Relative spectral transmission of different optical elements of the LSD.

Fig. 3 Overall relative spectral transmission curve of all optical elements shown in fig. 2, including a cold mirror in the light house beneath the film. This mirror is not shown in fig. 2.

Fig. 4 Relative and absolute spectral density distribution of an OSRAM Xenon arc lamp XBO 450 W.

Fig. 5 Relative spectral sensitivity curves for the fiducial PM XP 1110 and the track PM XP 1002.

Fig. 6 Example of the SCHNEIDER computer output concerning chromatic aberrations of the Repro-Claron 305mm, f:9; Left hand diagram shows "pulse width W" of 10µ for green light on the optical axis.

Fig. 7 Same as fig. 6. Right hand diagram shows chromatic variation of geometrical aberrations for a tangentially oriented step function at 160mm distance from the optical axis.

Fig. 8 Energy distribution in the 2.8x enlarged image of a 0%-100% step function and superposition of a step function with its inverse function to form the image of a line which is (in the object plane) of width $W_i/2,8$.

fig. 8a: case of a radially oriented line on the optical axis;

fig. 8b: case of a tangentially oriented line at a distance of 160mm from optical axis.

Fig. 9a Plot of "pulse width W" versus displacement of focal plane $\Delta s'$. The inserted numbers indicate off-axis distances in the image plane for green light (546nm, solid lines) and blue light (480nm, dashed lines).

Fig. 9b Conditions chosen from fig. 9a for operation of the LSD.
Wavelength of "fiducial light": 470nm;
Wavelength of "track light": 505nm.

Fig. 10 Reflectance curves for the small and large splitter.
Solid curves new mirrors;
Dashed curves - old mirrors.

Fig. 11 Final relative spectral sensitivity curve for the track PM XP 1002, S-20.
Solid curve - new mirror set;
Dashed curve - old mirror set;
dotted curve - proposed future improvement.

Fig. 12 Final relative spectral sensitivity curve for the fiducial PM XP 1110, S-11.
Solid curve - new mirror set;
Dashed curve - old mirror set;
Dotted curve - cut-away portion of the solid curve.

Fig. 13 Final relative spectral sensitivity curve for the vidicon.
Solid curve - with filter FILTRAFLEX DT-GRÜN;
Dashed curve - with filter FITC-3 special.

Fig. 14 Spectral distribution curve for the light falling on the operator's table.

Fig. 15 Spectral transmittance curves for the three BALZERS filters used in the LSD2.

Fig. 16 Residual reflectance of the second surface of a glass plate coated with three different types of AR coatings.
Solid curve - single layer of MgF_2 (SG5);
Dashed curve - double layer (short GEDO);
Dotted curve - multi-layer (short IRALIN).

Fig. 17 Sketch of the repartition of light in the LSD machines. Intensities of the primary and ghost images at the various places are given as fractions of the normalised incident light intensity.
Transmission through the small splitter: Operator's table;
Transmission through the large splitter: Fiducials and TV;
Reflection at the large splitter: Cone/periscope system.

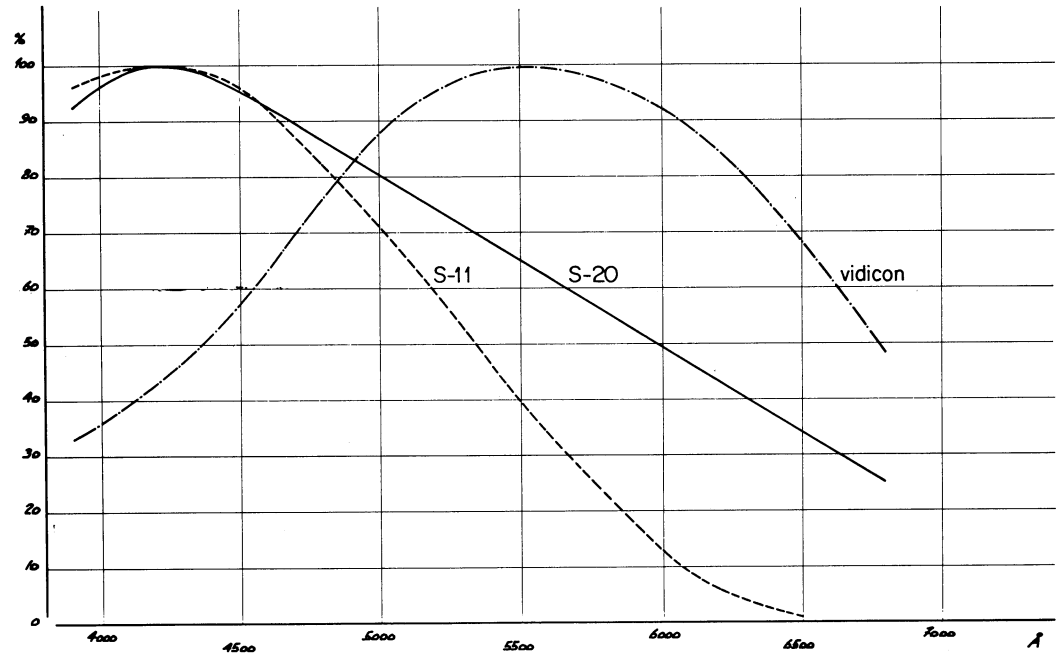
%
100
90
80
70
60
50
40
30
20
10
0
S-11
S-20
vidicon
4000
4500
5000
5500
6000
6500
7000
Å

Fig. 1

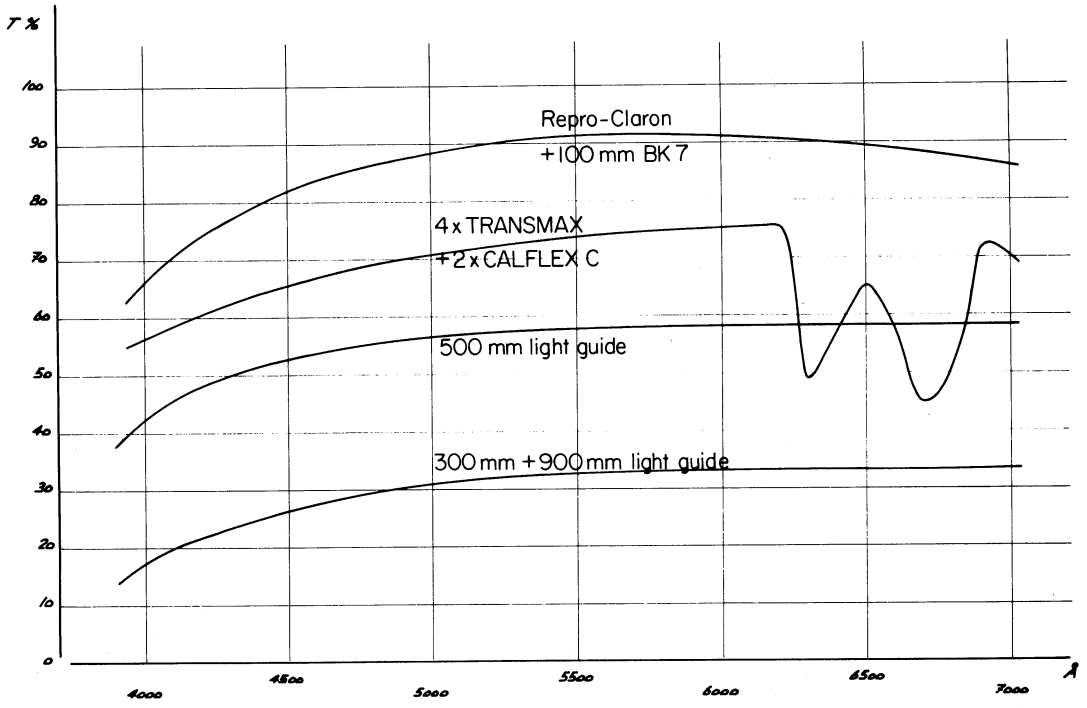
T %
100
90
80
70
60
50
40
30
20
10
0
Repro-Claron
+100 mm BK 7
4 x TRANSMAX
+2 x CALFLEX C
500 mm light guide
300 mm + 900 mm light guide
4000
4500
5000
5500
6000
6500
7000
Å

Fig. 2

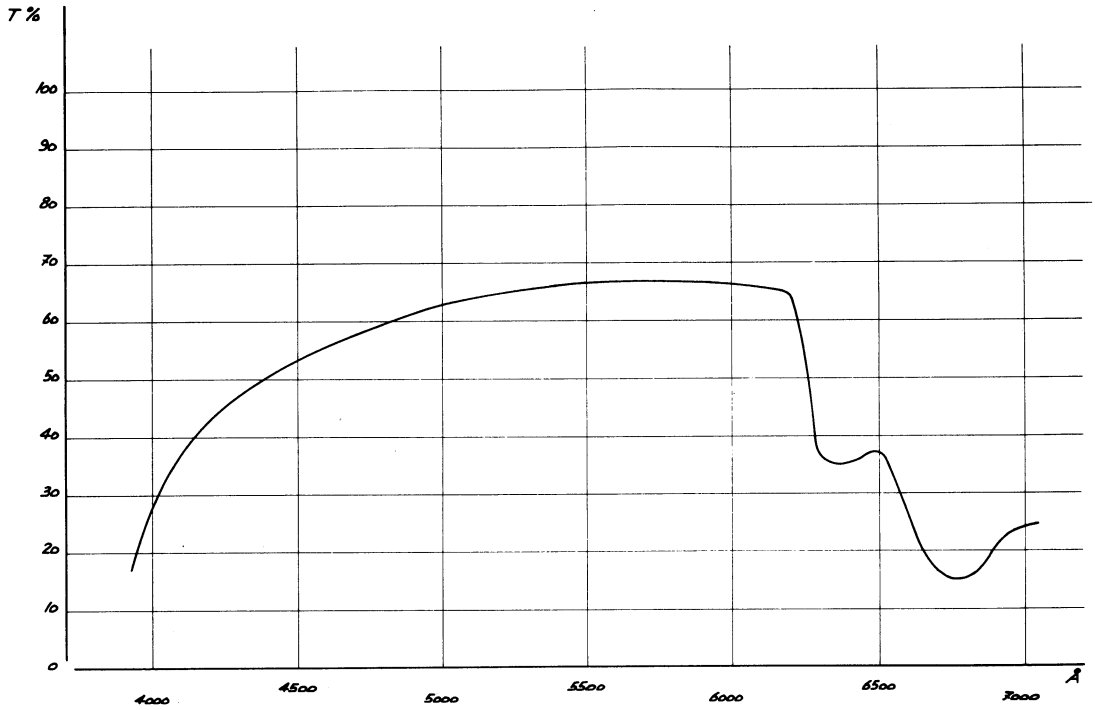
T %
100
90
80
70
60
50
40
30
20
10
0
4000
4500
5000
5500
6000
6500
7000
Å

Fig. 3

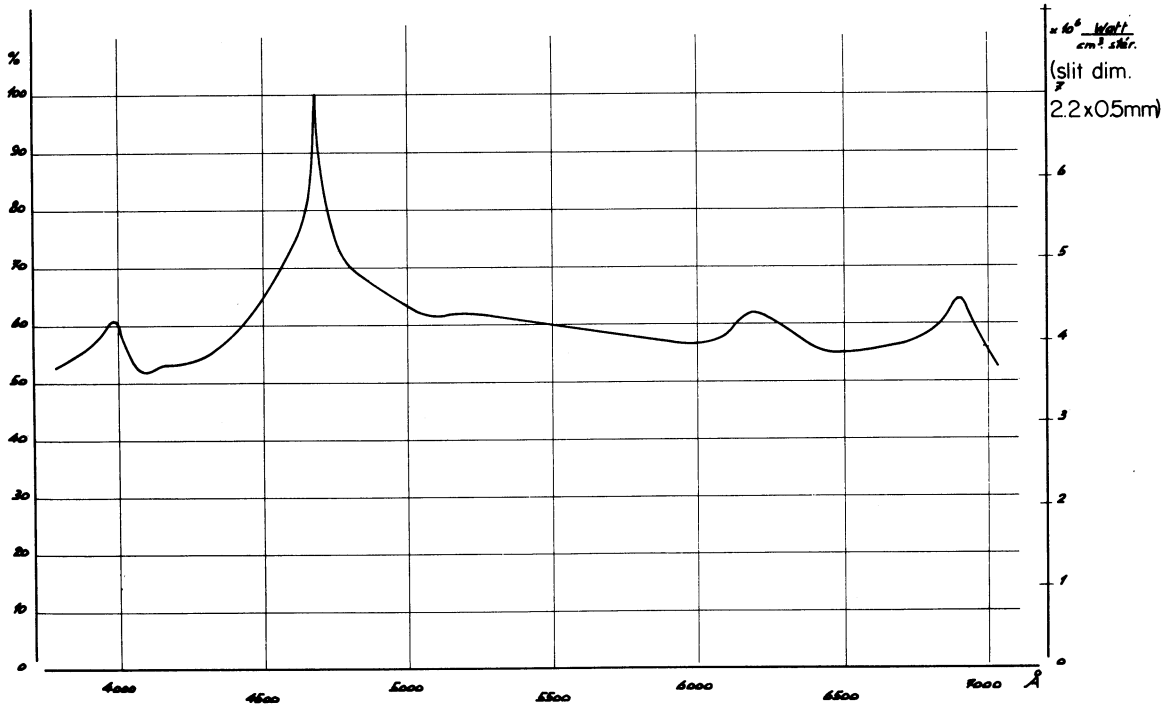
%
100
90
80
70
60
50
40
30
20
10
0
4000
4500
5000
5500
6000
6500
7000
Å
x 10⁶ watt / cm² steir.
(slit dim.
2.2x0.5mm)
6
5
4
3
2
1
0

Fig. 4

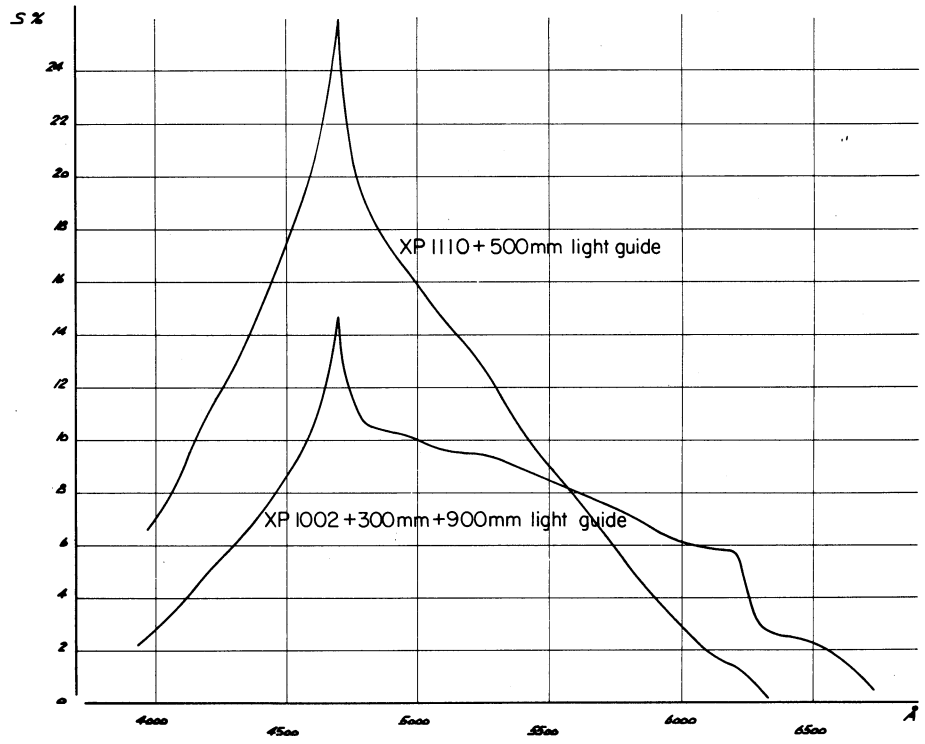
S %
24
22
20
18
16
14
12
10
8
6
4
2
0
XP 1110 + 500mm light guide
XP 1002 + 300mm + 900mm light guide
4000
4500
5000
5500
6000
6500
Å

Fig. 5

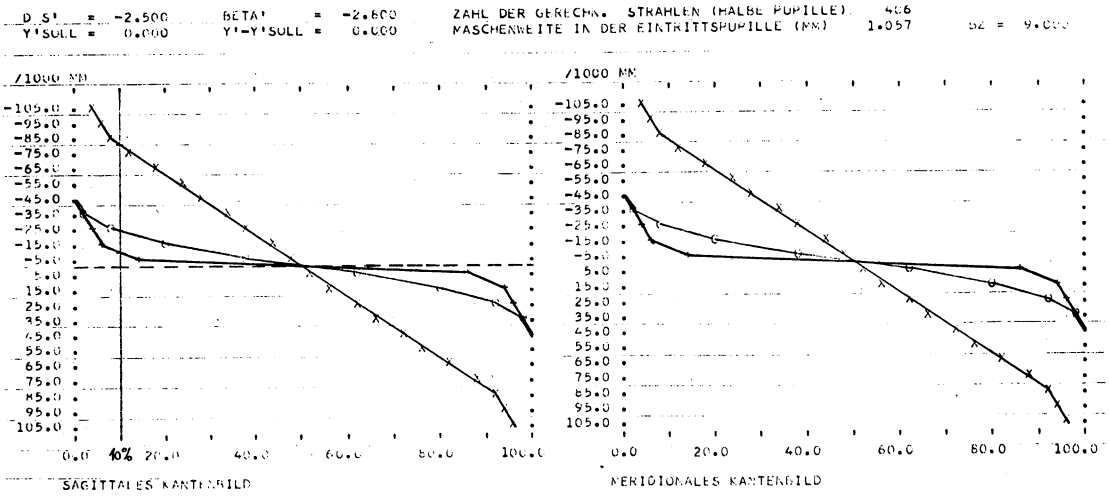
D S' = -2.500
Y'SOLL = 0.000
BETA' = -2.800
Y'-Y'SOLL = 0.000
ZAHL DER GERECHN. STRAHLEN (HALBE PUPILLE) 406
MASCHENWEITE IN DER EINTRITTSPUPILLE (MM) 1.057
/1000 MM
SAGITTALES KANTENBILD
MERIDIONALES KANTENBILD
+ = 546 nm
X = 644 nm
O = 480 nm

Fig. 6

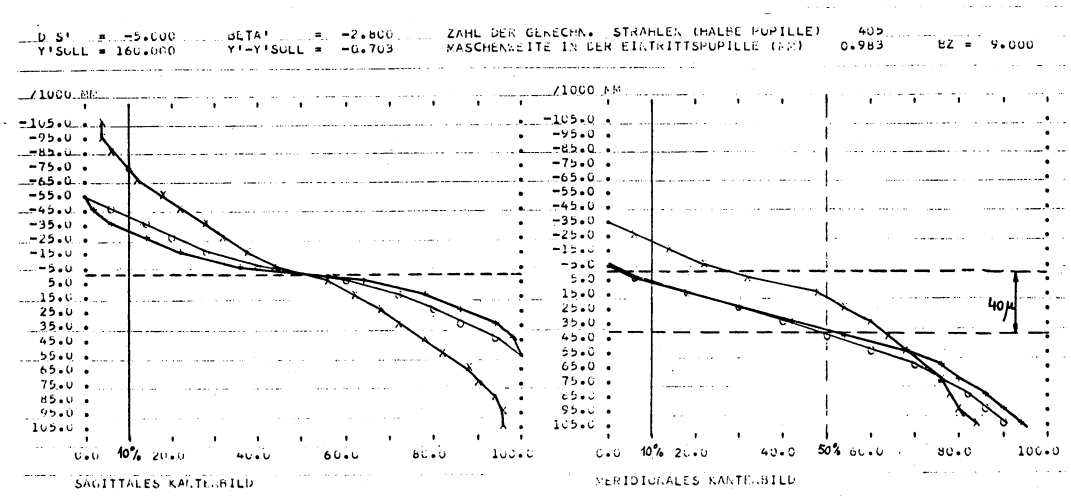
D S' = -5.000
Y'SOLL = 160.000
BETA' = -2.800
Y'-Y'SOLL = -0.703
ZAHL DER GERECHN. STRAHLEN (HALBE PUPILLE) 405
MASCHENWEITE IN DER EINTRITTSPUPILLE (MM) 0.983
BZ = 9.000
/1000 MM
40µ
SAGITTALES KANTENBILD
MERIDIONALES KANTENBILD
+ = 546 nm
X = 644 nm
O = 480 nm

Fig. 7

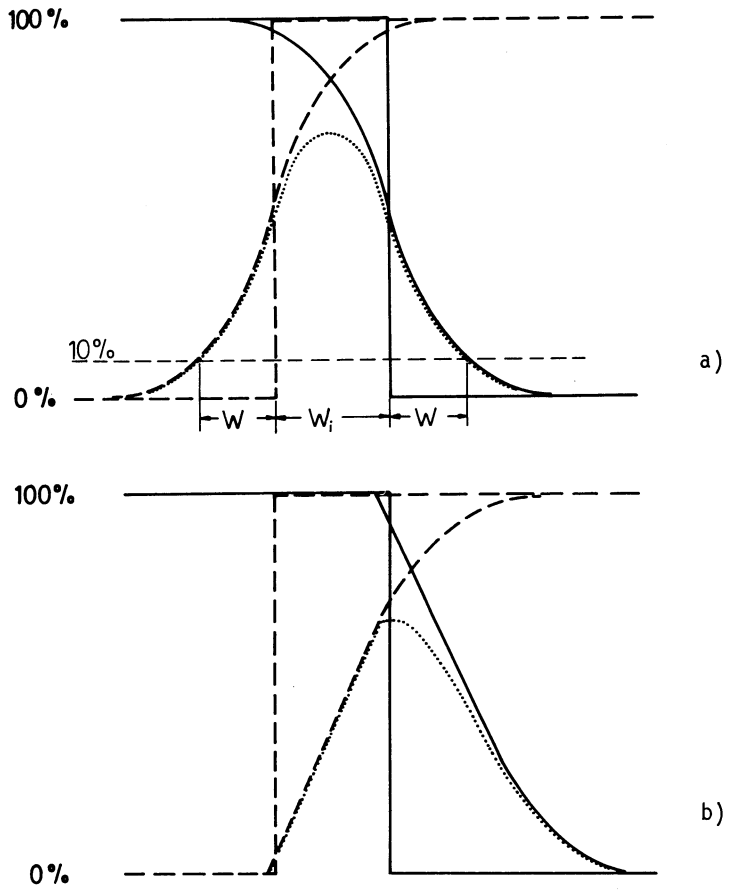
100 %
10%
0 %
W
Wi
W
a)
100%
0%
b)

Fig. 8

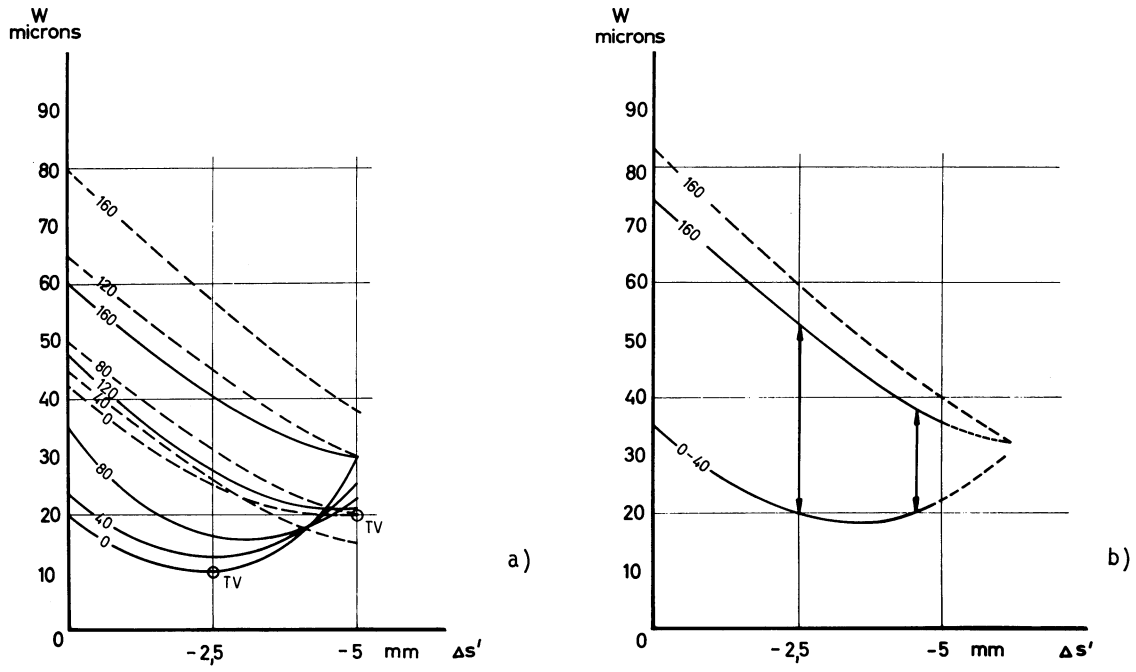
W
microns
90
80
70
60
50
40
30
20
10
0
160
120
160
80
120
40
0
80
40
0
TV
TV
-2,5
-5
mm
Δs'
a)
W
microns
90
80
70
60
50
40
30
20
10
0
160
160
0-40
-2,5
-5
mm
Δs'
b)

Fig. 9

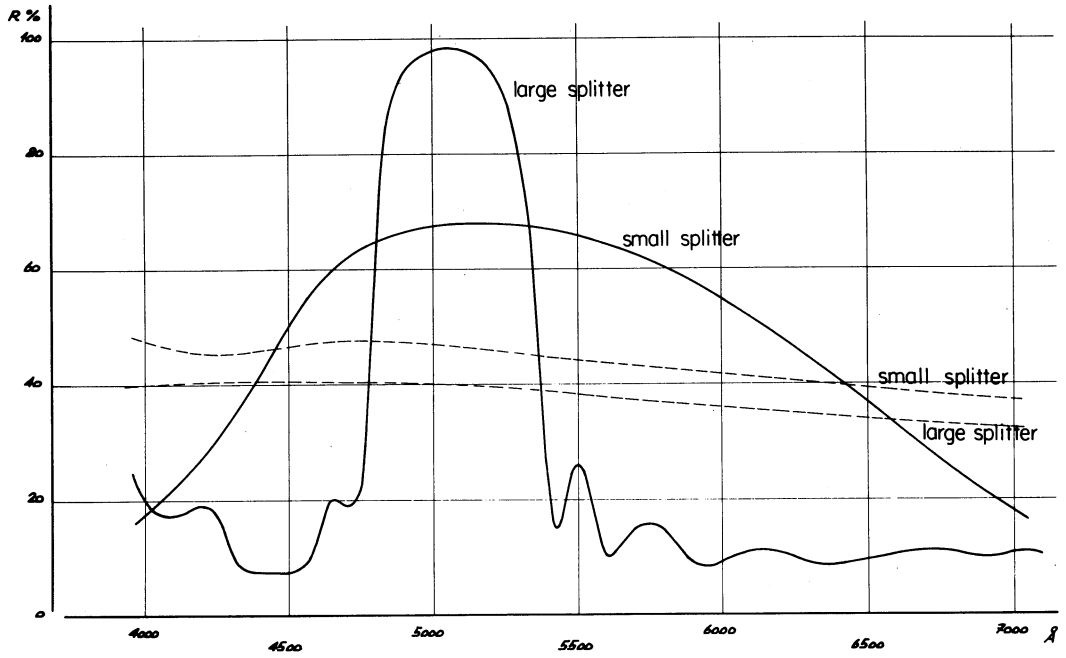
R %
100
80
60
40
20
0
large splitter
small splitter
small splitter
large splitter
4000
4500
5000
5500
6000
6500
7000
Å

Fig. 10

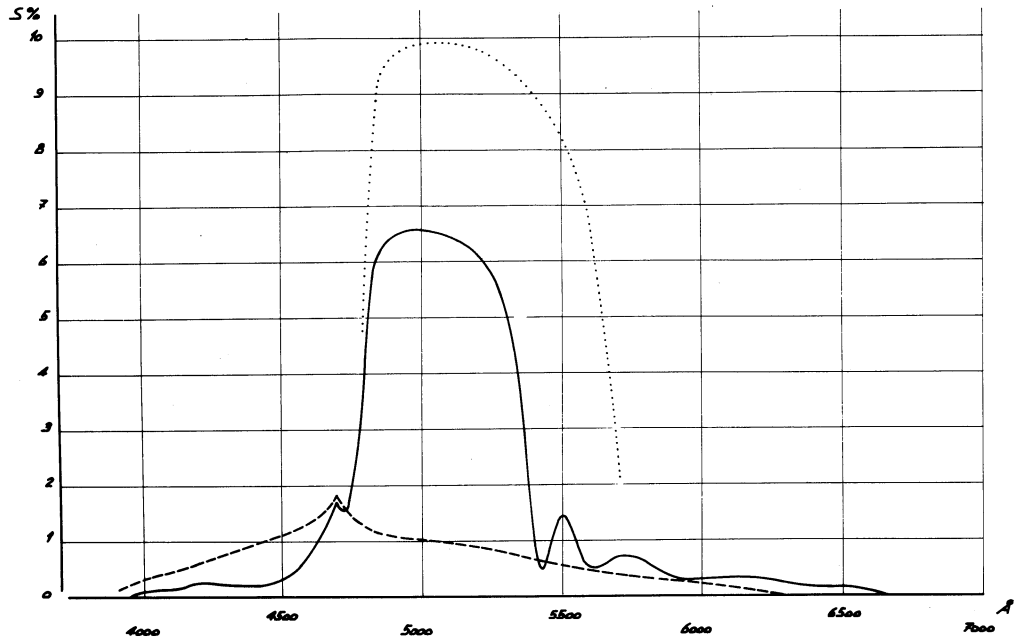
S %
10
9
8
7
6
5
4
3
2
1
0
4000
4500
5000
5500
6000
6500
7000
Å

Fig. 11

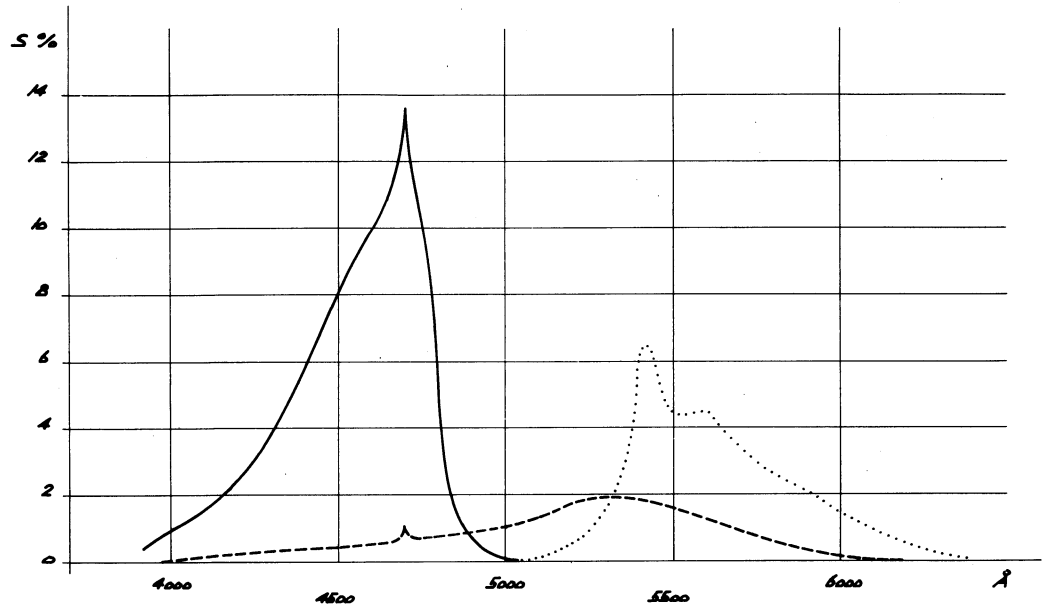
S %
14
12
10
8
6
4
2
0
4000
4500
5000
5500
6000
Å

Fig. 12

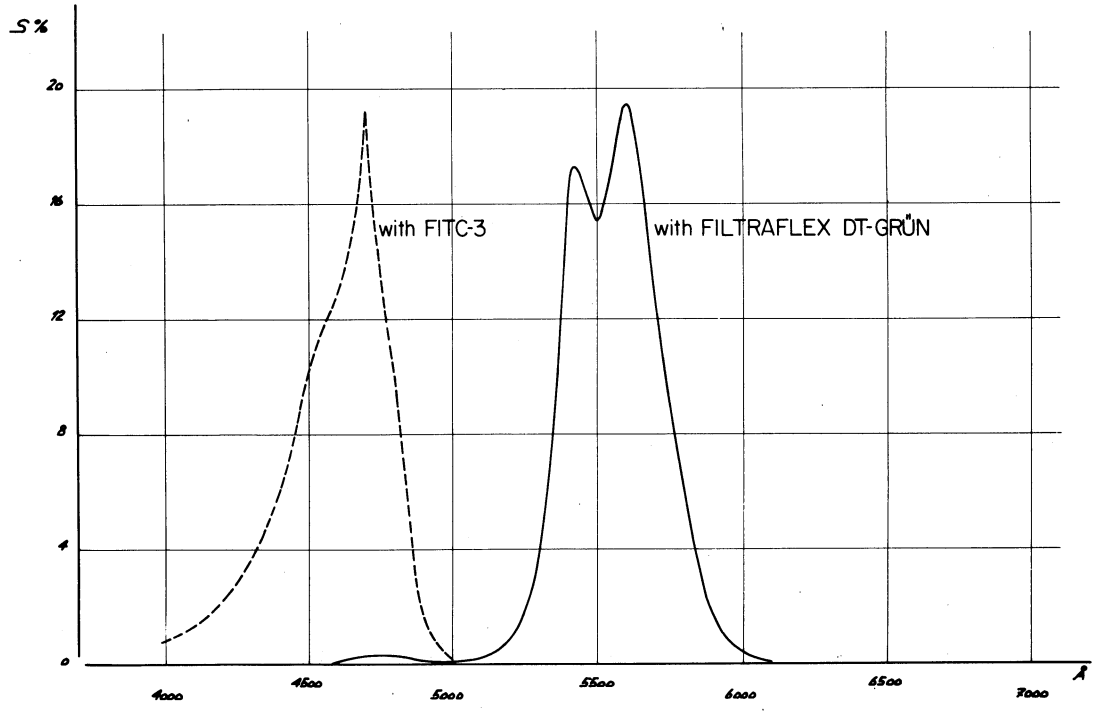
S %
20
16
12
8
4
0
with FITC-3
with FILTRAFLEX DT-GRÜN
4000
4500
5000
5500
6000
6500
7000
Å

Fig. 13

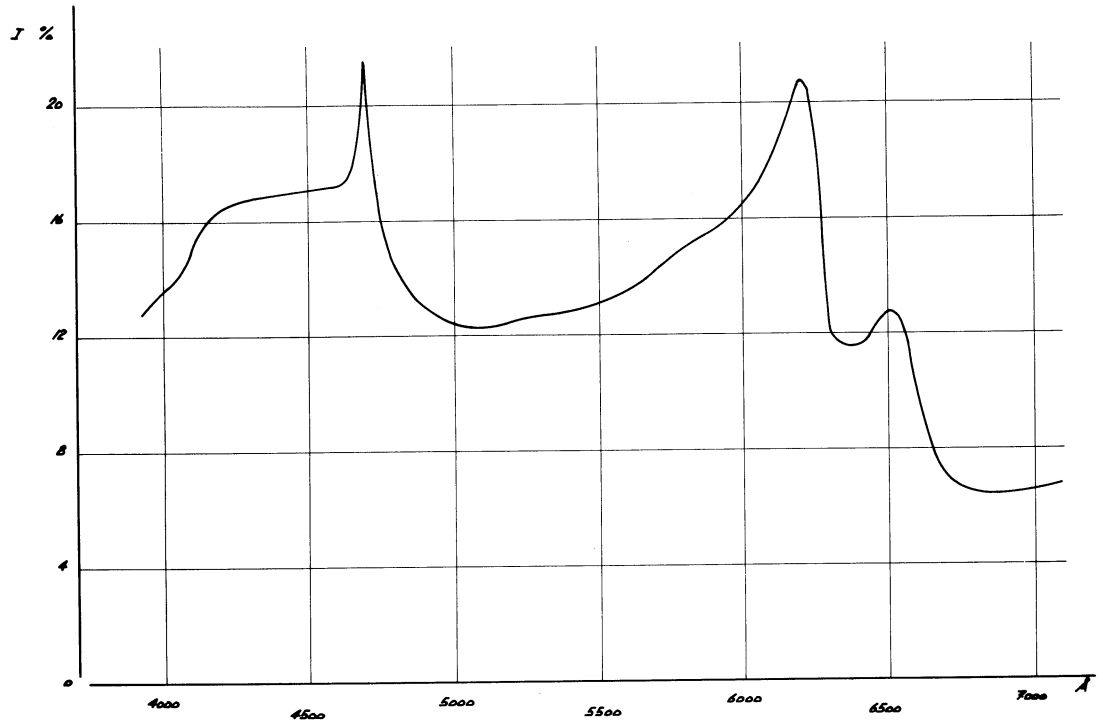
I %
20
16
12
8
4
0
4000
4500
5000
5500
6000
6500
7000
A

Fig. 14

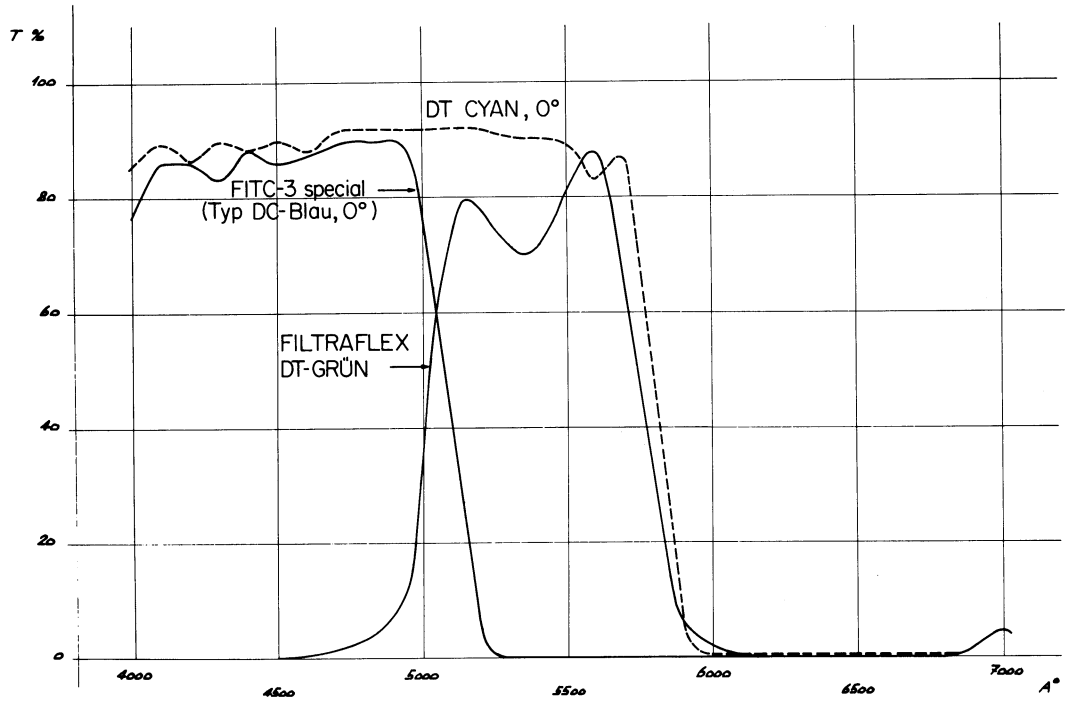
T %
100
80
60
40
20
0
DT CYAN, 0°
FITC-3 special
(Typ DC-Blau, 0°)
FILTRAFLEX
DT-GRÜN
4000
4500
5000
5500
6000
6500
7000
A°

Fig. 15

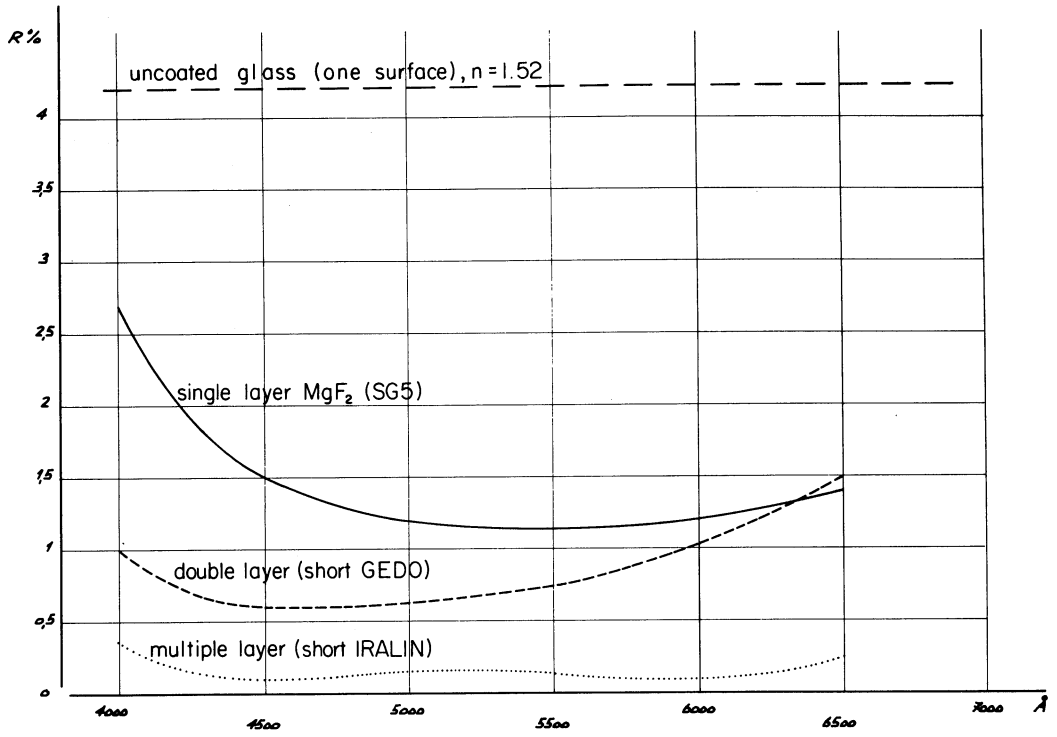
R %
uncoated glass (one surface), n = 1.52
single layer MgF_2 (SG5)
double layer (short GEDO)
multiple layer (short IRALIN)
4
3,5
3
2,5
2
1,5
1
0,5
0
4000
4500
5000
5500
6000
6500
7000
Å

Fig. 16

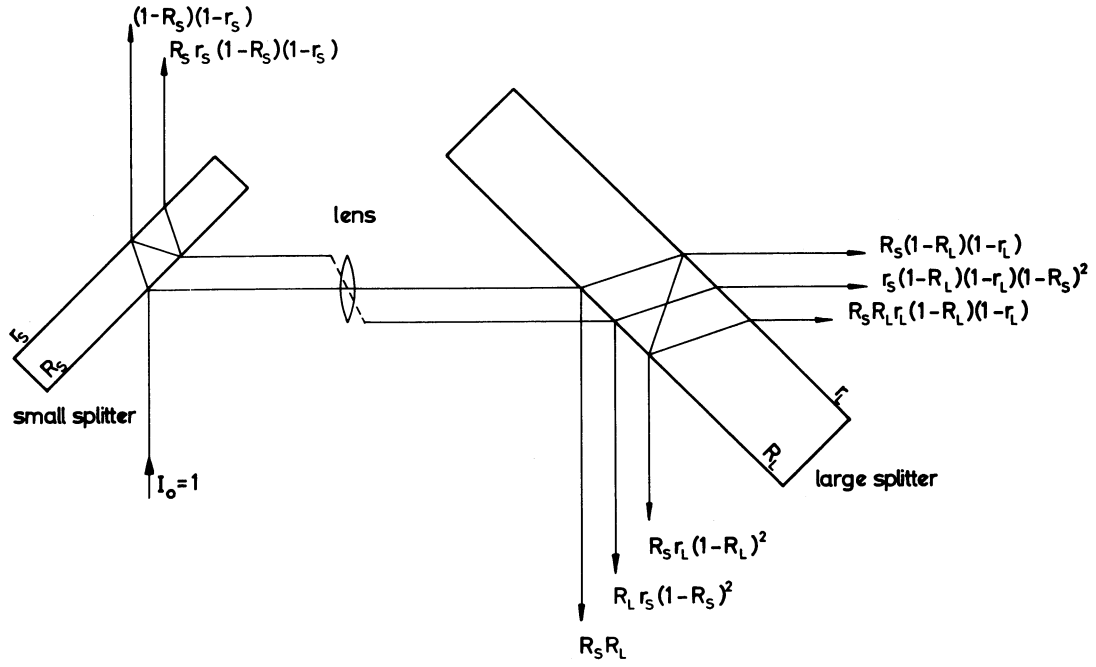
$(1-R_S)(1-r_S)$
$R_S r_S (1-R_S)(1-r_S)$
lens
$R_S(1-R_L)(1-r_L)$
$r_S(1-R_L)(1-r_L)(1-R_S)^2$
$R_S R_L r_L (1-R_L)(1-r_L)$
r_S
R_S
small splitter
$I_o=1$
r_L
R_L
large splitter
$R_S r_L (1-R_L)^2$
$R_L r_S (1-R_S)^2$
$R_S R_L$

Fig. 17